

Supporting Online Material for

p27^{kip1} stabilization is essential for the maintenance of cell cycle arrest in response to DNA damage

Myriam Cuadrado^{1,3}, Paula Gutierrez-Martinez^{1,3}, Aneta Swat², Angel R. Nebreda² and Oscar Fernandez-Capetillo^{1*}.

¹Genomic Instability Group; Spanish National Cancer Research Centre (CNIO); Madrid; 28029, Spain.

²Signalling and Cell Cycle Group; Spanish National Cancer Research Centre (CNIO); Madrid; 28029, Spain

³Equal contributors.

Note: M.Cuadrado and P. Gutierrez-Martinez share the first authorship.

*To whom correspondence should be addressed. Phone: +34-91-7328000 Ext: 3480. E-mail: ofernandez@cnio.es

Figure S1. p27 mRNA levels do not increase upon DNA damage. Q-RTPCR of p27 levels from A549 cells before and after a 24 hr exposure to Dox. Data were normalized with GAPDH levels. Data represent the mean and s.d. from three independent experiments.

Cuadrado et al Figure S1

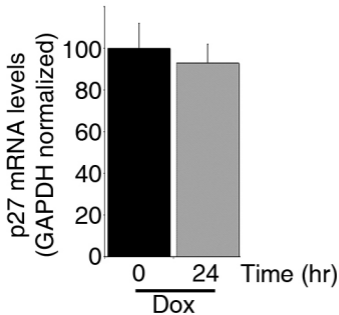


Figure S2. DNA Repair is not affected by p27 levels. (A) Reporter substrate for analysis of NHEJ. The reporter substrate consists of a split GFP with an artificially engineered intron, interrupted by an adenoviral exon, flanked by restriction sites for induction of DSBs. In this construct, the GFP gene is inactive; however, upon digestion with *HindIII* and successful NHEJ, the construct becomes GFP (1). (B) The percentage of successful NHEJ in p27^{wt} and p27^{low} cells was measured as described in (A) by transfection of a *HindIII*-linearized reporter substrate. The numbers represent the number of GFP cells, normalized for the transfection efficiency by co-transfection with a DsRed expressing plasmid (and relative to the levels found in p27^{wt} cells). (C) The image illustrates the dynamics of H2AX phosphorylation in p27^{wt} and p27^{low} cells that have been exposed to the radiomimetic drug neocarzinostatin for one hour (100ng/ml) and then released into drug-free media. Images were acquired by a High-Throughput microscopy platform each of the dots indicating the signal of γ H2AX per individual nucleus. (D) Examples from the analyses shown in (C). Scale bar (white) indicates 20 μ m.

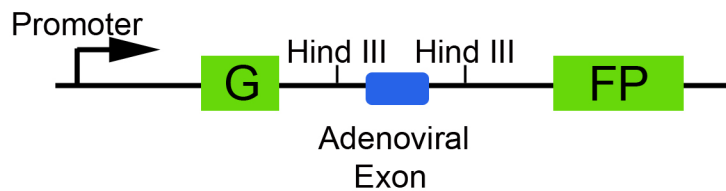
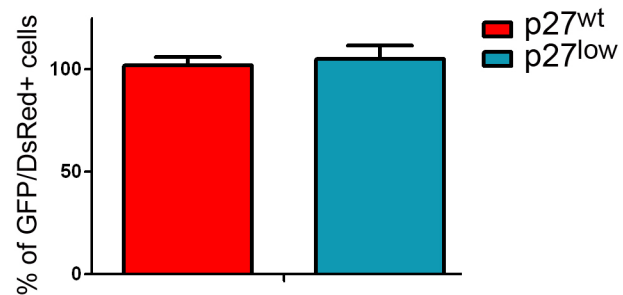
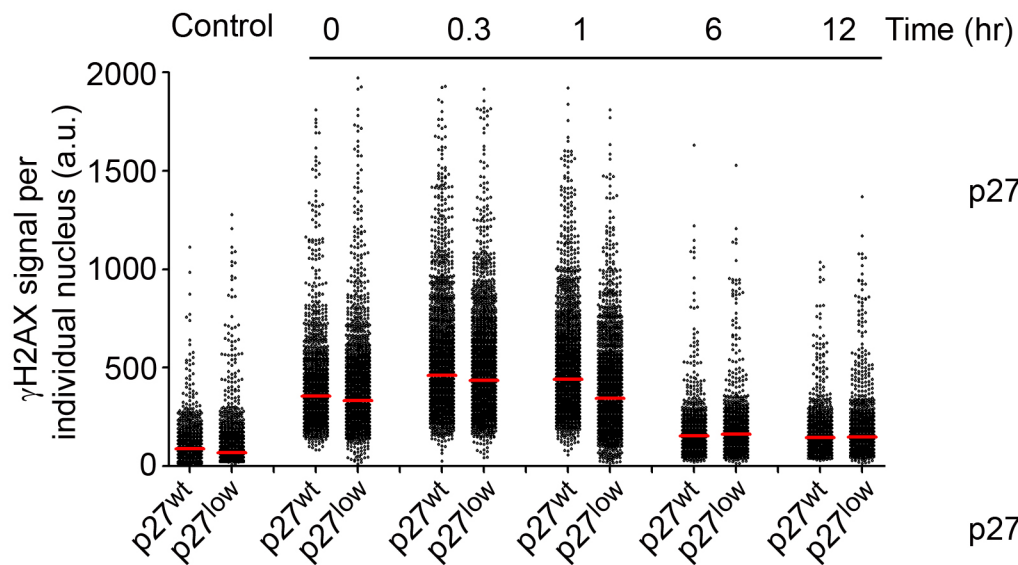
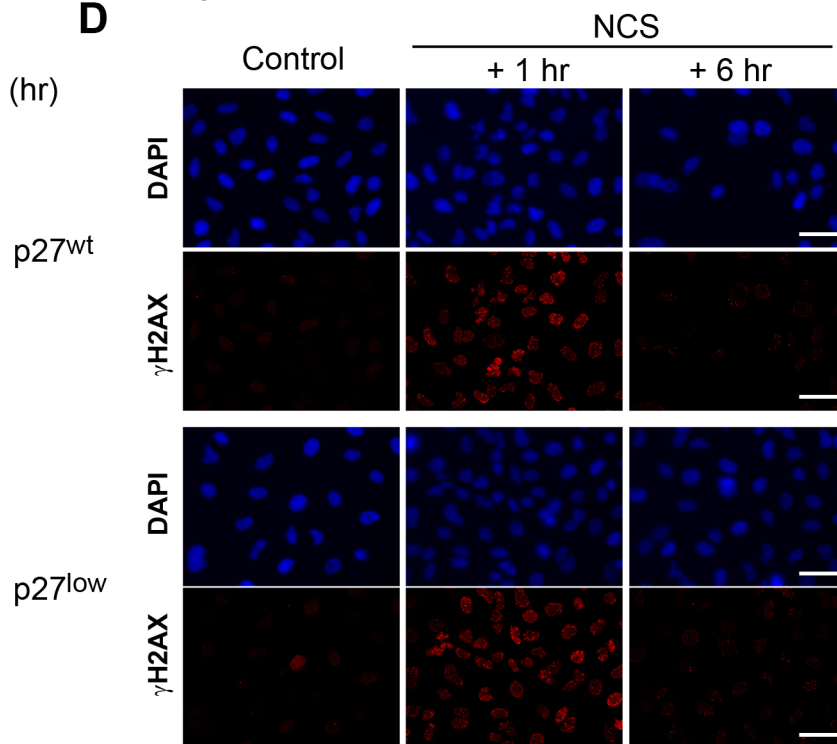
A**B****C****D**

Figure S3. p27 depleted cells enter S phase with DNA breaks. Immunofluorescence data of p27^{wt} and p27^{low} cells co-stained with γ H2AX (red) and EdU (green) in cells that have been exposed (or not exposed) to Dox for 24 hrs and then released for another 24 hrs in drug-free medium. White arrows indicate cells in S phase (EdU positive) in each of the conditions. Scale bar (white) indicates 10 μ m.

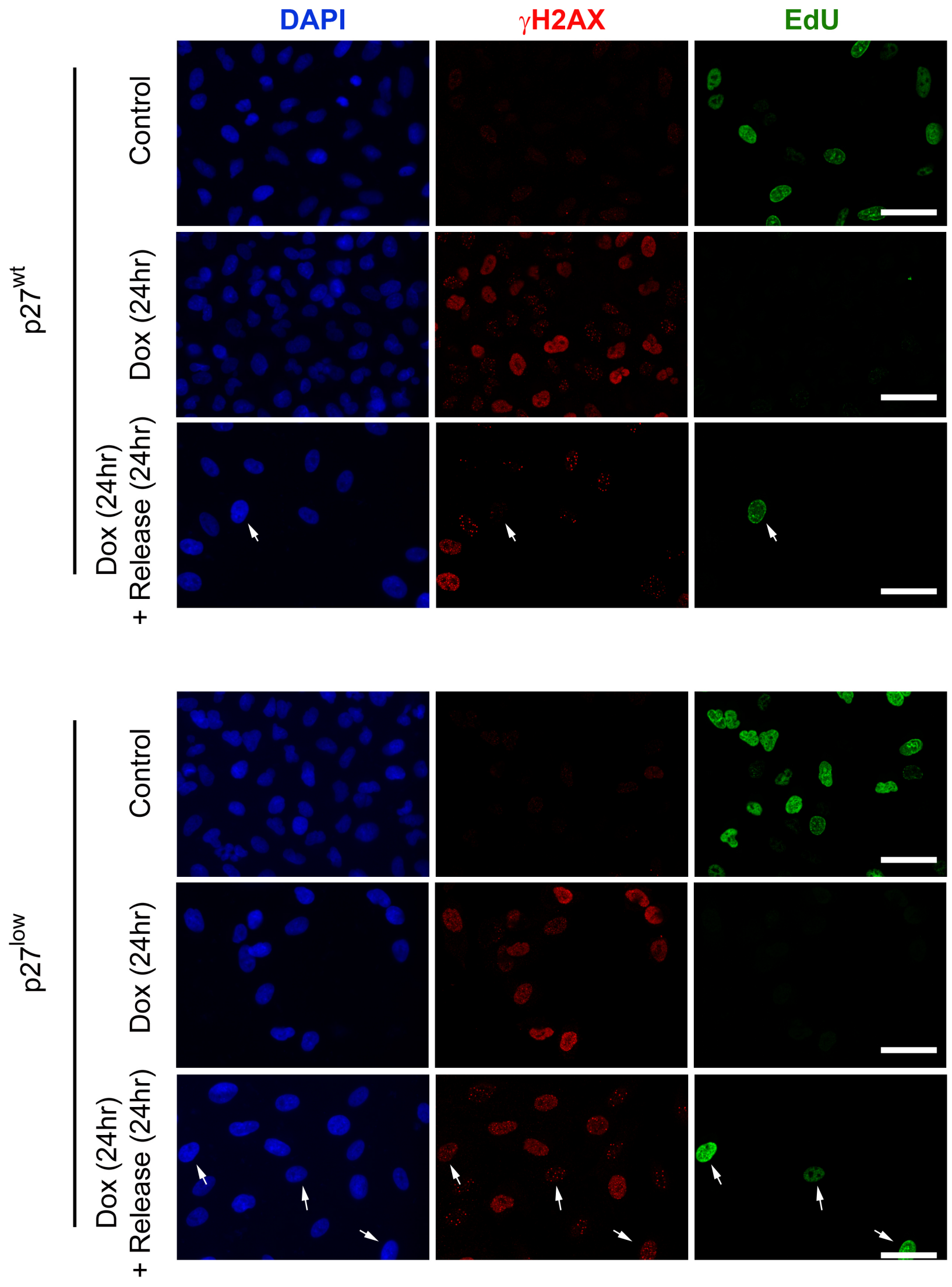


Figure S4. Chromosomal abnormalities found in p27^{low} cells. The figure provides several examples of Giemsa stained karyotypes illustrating the chromosomal abnormalities that were found on p27^{low} cells upon exposure to Dox for 24 hrs and then released for another 24 hrs in drug-free medium (as shown, no abnormalities were observed in either treated or untreated p27^{wt} cells or untreated p27^{low} cells). The most frequent observation was chromosomal fragments (as indicated by red asterisks).

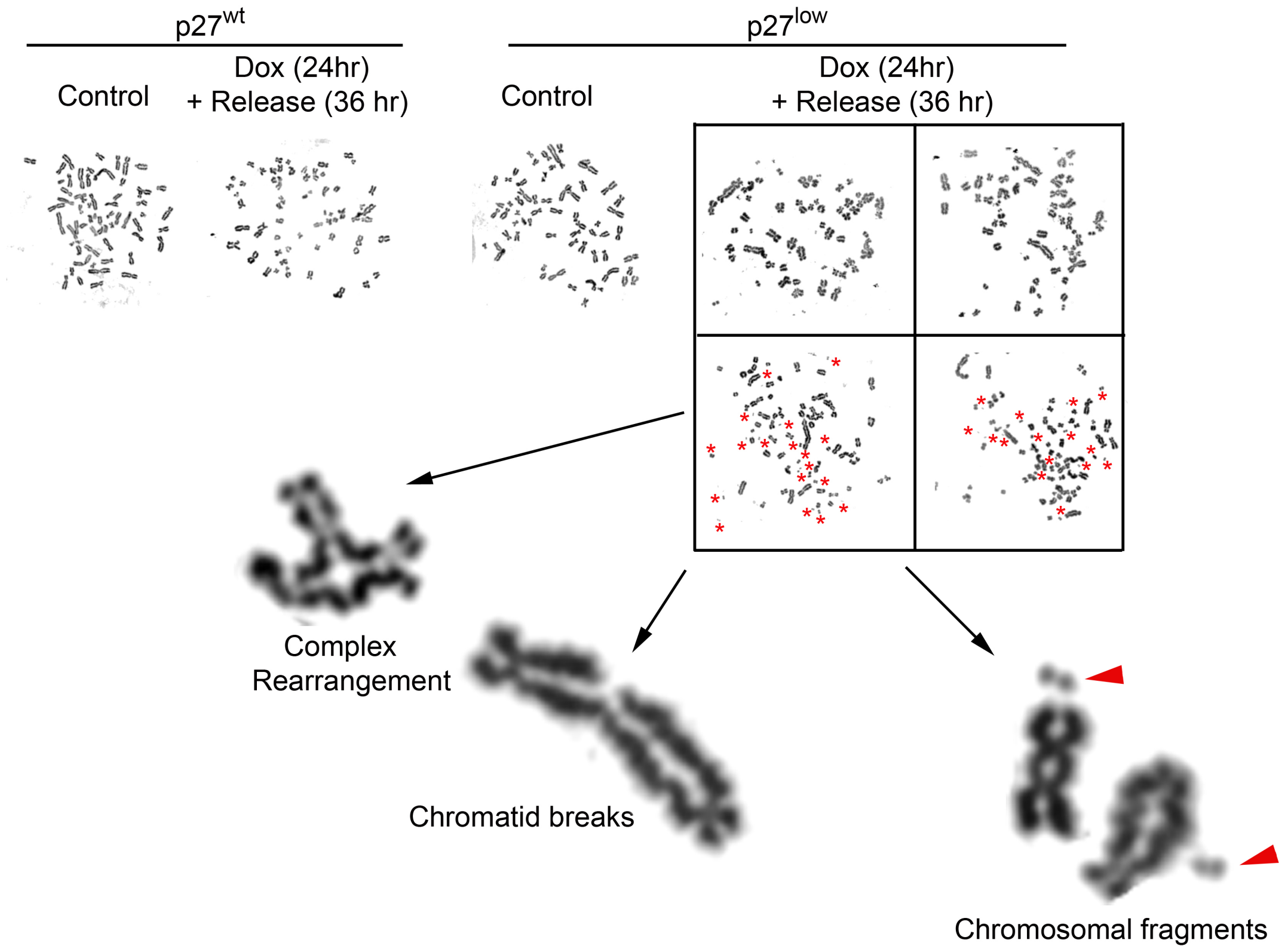


Figure S5. Putative ATM/ATR phosphorylation sites on p27. Schema illustrating the presence of putative ATM/ATR sites (red balls) on the N-terminus of p27 (as identified on www.scansite.edu). Note that such potential sites are located exclusively in almost every peak of surface exposed regions of the N-terminus.

Cuadrado et al Figure S5

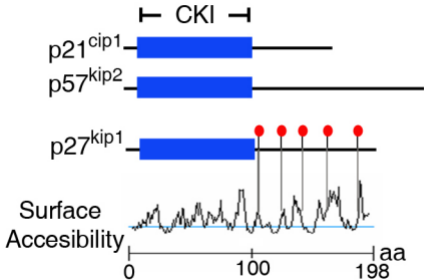
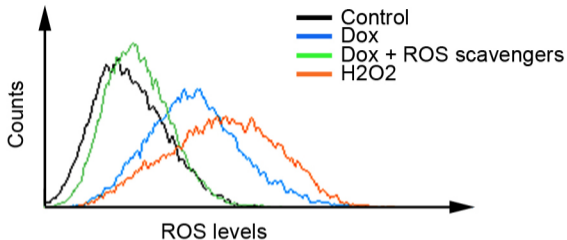
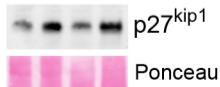


Figure S6. DNA damage induced ROS does not mediate p27 stabilization. (A) The levels of ROS were detected by flow cytometry with the ROS-detecting probe 2',7'-dichlorodihydrofluorescein diacetate. Cells were treated with Dox for 24 hrs as in the rest of the experiments shown, in the absence or presence of the ROS scavengers L-Glutathion and N-acetyl-Cysteine (both at 5mM). As shown, the dose used for the ROS scavengers is able to eliminate the levels of ROS induced by the Dox treatment. As a positive control, cells were treated with 5mM H₂O₂ for 6 hrs. (B) Western blot illustrating the levels of p27 on A549 exposed to Dox for 24 hrs, in the absence or presence of the ROS scavengers L-Glutathion and N-acetyl-Cysteine at the doses used in (A).

A**B**

ROS scavengers	-	-	+	+
Dox (24 hr)	-	+	-	+



SUPPLEMENTARY METHODS

NHEJ Assay. The assay used to specifically measure NHEJ was described in (1). In brief, the NHEJ reporter plasmid was digested with *HindIII* for 6 h and purified by using a Qiagen gel extraction kit. Aliquots were analyzed by gel electrophoresis to confirm complete digestion. 10^6 cells were transfected with 1 μ g of predigested NHEJ reporter substrate along with 1 μ g of pDsRed2-N1 (Clontech) to serve as transfection control. Expression of GFP and DsRed was monitored by FACS 48 hrs after transfection.

Immunofluorescence and HT microscopy. The HT-microscopy mediated analysis of γ H2AX has been described before (2). Briefly, cells were grown on μ CLEAR bottom 96 well dishes (Greiner Bio-One), and analyzed on a BD PathwayTM 855 BioImager (Beckton Dickinson). Image analysis was performed with the AttoVision software (Beckton Dickinson). All the images for quantitative analyses were acquired under non-saturating exposure conditions. γ H2AX antibodies (Upstate Biotechnology) together with secondary antibodies conjugated with Alexa 488 (Molecular probes) were used. For EdU and γ H2AX immunostainings, *Click-IT EdU* was used according to manufacturer's instructions (Invitrogen).

Analysis of ROS levels. Intracellular ROS levels were measured with the ROS-reacting dye 2',7'-dichlorodihydrofluorescein diacetate (SIGMA). Briefly, after treatment cells were washed in PBS and incubated at 37°C for 10 min with a PBS-buffered solution containing 5.5 mM glucose and 10 μ M of the probe. Cells were then washed in PBS, fixed for 10 min in 4% paraformaldehyde and finally suspended in PBS before going to the cytometer.

SUPPLEMENTARY REFERENCES

- 1. Seluanov A, Mittelman D, Pereira-Smith OM, Wilson JH, Gorbunova V. DNA end joining becomes less efficient and more error-prone during cellular senescence. Proc Natl Acad Sci U S A 2004; 101: 7624-9.**
- 2. Murga M, Jaco I, Fan Y, et al. Global chromatin compaction limits the strength of the DNA damage response. J Cell Biol 2007; 178: 1101-8.**